

University of Arkansas, Fayetteville
ScholarWorks@UARK

Biomedical Engineering Undergraduate Honors
Theses

Biomedical Engineering

5-2017

In vivo multi-parametric imaging of metastatic and non-metastatic breast cancer

Raisa B. Rasul
University of Arkansas

Follow this and additional works at: <http://scholarworks.uark.edu/bmeguht>

 Part of the [Bioimaging and Biomedical Optics Commons](#)

Recommended Citation

Rasul, Raisa B., "In vivo multi-parametric imaging of metastatic and non-metastatic breast cancer" (2017). *Biomedical Engineering Undergraduate Honors Theses*. 48.
<http://scholarworks.uark.edu/bmeguht/48>

This Thesis is brought to you for free and open access by the Biomedical Engineering at ScholarWorks@UARK. It has been accepted for inclusion in Biomedical Engineering Undergraduate Honors Theses by an authorized administrator of ScholarWorks@UARK. For more information, please contact scholar@uark.edu, ccmiddle@uark.edu.

Abstract

A current issue in cancer therapy is the characterization of metastatic tumors, which can increase ease of treatment and patient trials. We present an in vivo study of metastatic (4T1) and non-metastatic (4T1-TWIST KO) breast tumor sister cell lines to understand their metabolic behavior, determine differences in two modes of imaging (reflection & transmission), and observe effect of breathing higher oxygen percentage on vascular hemoglobin oxygen saturation. After injection of 10,000 cells into mice dorsal window chambers, the glucose intake and hemoglobin oxygen saturation was measured using a fluorescent glucose analog (2-NBDG) and hyperspectral trans-illumination imaging from 520-620 nm at 10 nm intervals, respectively. The metastatic tumors exhibited increased oxygen saturation and decreased glucose metabolism than non-metastatic tumors. Reflection mode of imaging was unable to pick intricacies in tumor parameters, and increased inhalation of oxygen caused increase in hemoglobin oxygen saturation.

Introduction

Approximately 90% of cancer deaths are caused not by primary tumors but the metastases that spread from these primary tumors and invade other areas of the body^{1,2}. Current methods of treating cancer include surgical resection and adjuvant therapy, such as radiation or chemotherapy, to prevent future reoccurrences of the disease. Early detection of metastatic or malignant cancer can improve not only patient mortality and ease but can also decrease the economics burden of unnecessary cancer treatments and working age people who are unable to work. According to the cancer plan of 2011 made by the Department of Health of the United Kingdom, many general physicians say that access to diagnostic tests that identify cancer or exclude cancers earlier is an important issue that they want to be addressed³. Other doctors agree that early detection can prevent increased costs that come with subsequent future treatment⁴.

It is not possible to give the same treatment for metastatic cancer to all cancer patients as it can increase costs and require the patient to be hospitalized for a longer period. Cancer treatments includes expensive agents, some of which are bevacizumab, cetuximab, irinotecan among others⁵. Over an 8-week course, the cost for only the agents can range from \$10,000 to \$30,000⁵. Patients will also unnecessarily suffer the toxic side-effects of chemo or radiotherapy. Patient's ease and economic impact combined indicate that it's important to understand and be able diagnose metastatic from non-metastatic cancers.

Breast cancer one of the most common metastatic cancers, especially among western women. Although the mechanism behind cancer metastatic is complex,

previous studies have indicated that cancerous cells exhibits increased glucose uptake and metabolism compared to non-cancerous cells^{6,7}. The enhanced expression of glucose transporters GLUT1 and GLUT3 observed in cancerous cells indicating a method of absorbing glucose⁷. Glucose plays a major role in the cellular respiration pathways, glycolysis, where a molecule of glucose is broken down into two molecules of pyruvate and a net total of two ATP molecules are formed. When oxygen is present, also known as aerobic respiration, the two pyruvate molecules are catabolized further through oxidative phosphorylation until an additional net 30 molecules of ATP are produced⁸. The presence of ATP is important especially for performing the cellular work involved in the metastasis process where cells have to break away from the extracellular matrix and the basement membrane to enter the bloodstream. Despite the advantage of more ATP molecules being produced in oxidative phosphorylation, cancer cells undergo high glycolytic metabolism and therefore enhanced glucose consumption, which can be detected through fluorescence imaging. One reason behind the upregulation of glycolysis might be due to obtaining an acidic tumor microenvironment, and then developing a resistance to the toxicity, a change which allows dominance of phenotypes such as cell proliferation and invasion⁹.

Another factor of the tumor microenvironment which can be imaged is how saturated the hemoglobin molecules of the red blood cells are with oxygen. Oxygenation of the tumor microenvironment is key because low oxygen levels, also known as hypoxia, can influence therapy resistance or metastasis of cancer cells^{10,11}. While there may be many factors controlling the metastatic outcome, one theory is that the metabolism of cancer cells can be explained by the hemoglobin oxygen saturation

of the tumor microenvironment, because the presence of oxygen general determines whether oxidative phosphorylation will take place or not.

The goal of our study was to compare changes in glucose metabolism and hemoglobin oxygen saturation between metastatic and non-metastatic cell lines, determine whether a fluorescence microscope can obtain both trans-illumination and reflection mode images using the same field of view, and identify the effect inhaling more oxygenated air on the hemoglobin oxygen saturation measurement. Utilizing those measurements, we want to develop a model for diagnosing metastatic breast cancer cell lines from non-metastatic ones. The panel of cell lines in the study include, 4T1, a murine breast cancer tumor, and its derivative 4T1-TWIST KO, which is the identical to 4T1 with the exception of having the TWIST gene deleted. TWIST is one of the genes thought to cause metastatic phenotypes in tumors through the process of epithelial to mesenchymal transition, therefore, the 4T1 cells with the TWIST gene are metastatic while the 4T1-TWIST KO cells without the gene are theoretically non-metastatic. We measured glucose consumption of these cell lines using 2-[N-(7-nitrobenz-2-oxa-1,3-dioxol-4-yl)amino]-2deoxyglucose (2-NBDG), a fluorescent analog of glucose, that was injected intravenous of the mouse tail. The hemoglobin oxygen saturation was measured through hyperspectral trans-illumination imaging of tumors in window chambers.

The amount of light absorbed in a mixture is determined by three factors, the absorption coefficient of the different components in the mixture, the concentration of the components, and the thickness of the sample. This principle is stated by the Beer Lambert Law, $A = \epsilon cl$, where A is the percent of light absorbed, ϵ is the absorption

coefficient, and l is the thickness of the sample. If light is shined onto a tumor while it is inside a mouse, some major components absorbing the light will be deoxygenated hemoglobin, oxygenated hemoglobin, and melanin (the pigment of in skin). Some wavelengths of light are better absorbed than others depending on the element that is absorbing. Figure 1. below display how the molar extinction coefficient of oxygenated and deoxygenated hemoglobin change as different wavelengths of light are absorbed.

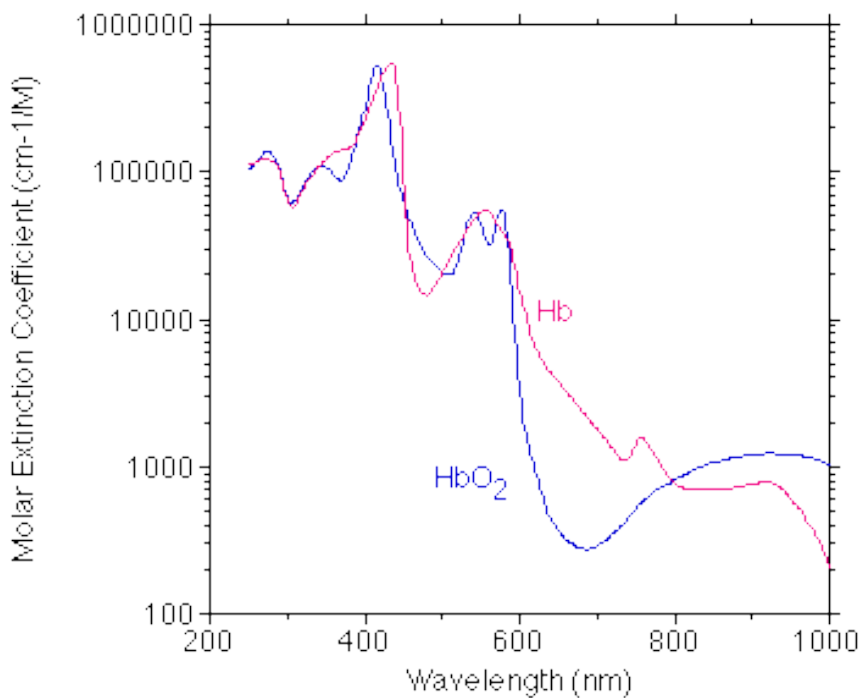


Figure 1. Hb (oxygenated hemoglobin) and HbO₂ (deoxygenated hemoglobin) have different molar extinction coefficients at varying wavelengths of light¹².

The measurement of the glucose uptake and hemoglobin oxygen saturation might help identify changes in tumor microenvironment between metastatic and non-metastatic cells.

Methods

Glucose uptake was measured through reflectance mode fluorescence imaging and hemoglobin oxygen saturation was measured using trans-illumination imaging on a bright field microscope. To see whether it's possible to obtain the same field of view for metabolism and oxygen saturation images, reflection mode and transmission mode images were taken of same field of view and the differences in the optical parameters were observed. A small difference would mean that that is possible to obtain hemoglobin oxygen saturation images in reflection mode and thus the same field of view in one microscope can be used. Finally, to understand the changes in the oxygen saturation, the increased oxygenated air was inhaled by the mouse to see whether an increase is also observed in the measured vascular oxygen saturation.

Window Chamber Surgery

To observe glucose metabolism and vascular oxygen saturation in vivo, cancer cells were injected into a mouse and the growing tumor was imaged subsequently. The type of surgery to inject the cells is called the dorsal skinfold window chamber and an imaged in shown in Figure 2. The strain of mice used was the female BALB/c and to prepare for the surgery, the mouse is shaved of its hair and the remaining hair is removed from the surgery areas using hair removal cream. During the period of hair removal, the mouse is under anesthesia and breathing in isoflurane for a period of 20 minutes. The mouse is allowed to wake up from the anesthesia before it is injected with approximately 100 ul of an anesthetic that consists of a 1:1:4 ratio of ketamine to

xylazine to saline solution and allows freedom of movement while the window chamber is placed.

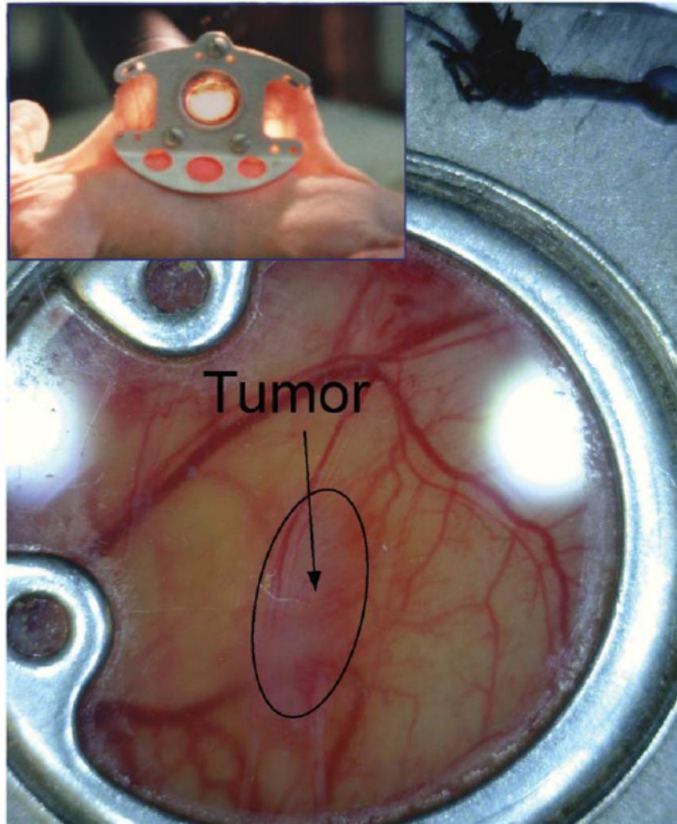


Figure 2. Dorsal skinfold window chamber¹³.

After the mouse goes under, it is placed on a heating pad covered with a sterile pad, and a surgical marker is used to draw points on the dorsal skinfold so that they match with the placement of the prongs on the window chamber. A metal punch is used to puncture the skin on the marks, and the three prongs of the window chamber is pushed through. To stabilize the other side of the chamber, a counterpart frame with

corresponding holes is pushed through

the prongs and the two frames are stabilized using bolts.

Using a surgical tweezer and scissor that is bent at the tip, the skin inside the window chamber with the smaller hole is cut out while making sure not to cut the skin on the opposite side. Approximately 10 μ l of cancer cells in a PBS solution with a concentration of 1x10⁶ cells/ml are injected into the fascial membrane of the skin that is present after the cut. The tip of a 30 gauge needle is bent before injecting the cells to decrease the chance of the needle puncturing the skin on the other side. After injection, the area around the cut is filled with saline using a needle, and a glass coverslip is

gently placed so that it's resting on top of the thin layer of saline. A stabilizing ring is firmly but moderately pressed on top of the glass coverslip to prevent it from falling out and sealing the cut from the outside environment. Putting too much pressure while placing the ring can break the coverslip.

After the mouse has recovered from the anesthesia, it is injected subcutaneously with approximately 60 μ l of Rhimadyl solution, an analgesic. Following signs of activity and movement, the mouse is placed back inside its cage. Sterile techniques are performed during the procedure and the mouse is housed in a facility that provides routine light-dark cycles.

Hyperspectral Hemoglobin Oxygen Saturation Measurement

On the second day after surgery, the mouse is imaged for hemoglobin oxygen saturation using a trans-illumination bright-field imaging microscope. The mouse is placed under anesthesia while it is on the microscope stand. A small nose cone and tubing is utilized to deliver the anesthetic gas from the chamber to mice. While it is under, the mouse is also breathing in 20% oxygenated air. A 3-D printed microscope slice, with holes cut out to match the three prongs of the window chamber is inserted onto the window chamber and stabilized with a bolt. The mouse is placed on the stand such that the glass coverslip in the chamber is facing the side of microscope with the camera. A liquid crystal tunable filter (LCTF) is used to filter the light obtained by the camera such that only a single wavelength of light is able to reach the camera. The tumor area is imaged using 4x magnification from wavelengths of 520nm to 620nm in

10nm increments. Exposure times are changed depending on the intensity saturation of the images and are noted down for calibration imaging.

Afterwards, the mouse is removed from microscope stand and anesthesia and placed back in its cage. Since exposure times can vary depending on wavelength, day of imaging or mice, the images were calibrated by taking background images with no mice on the stand at the same exposure times and the corresponding wavelengths. A dark image, with the microscope lamp covered is also obtain to factor in the effect of background light on the image intensity. Neutral density filters are used to decrease the intensity of all the calibration images because, the images will be extremely saturated if nothing is blocking the light from going to the camera. A MATLAB code is used to process the images, which subtracts the dark and calibration images from the original images and compares the intensity of the pixels at different wavelengths using the Beer Lambert Law to extrapolate the concentration of oxygenated hemoglobin. Hemoglobin oxygen saturation imaging is continued until tumor grows too large.

Reflection mode images were obtained by placing a lamp near the microscope such that the light is coming from the same side as the camera. After trans-illumination imaging, the mouse was kept on the stand and the additional lamp was placed, to have a constant field of view between the two different modes of imaging. During reflection imaging, the shutter of the microscope was closed to prevent the halogen lamp from sending transmitted light to the camera. Reflection and transmission images were taken at 4x, 10x, and 20x magnifications since most 2 photon microscopes have a single 20x objective but hemoglobin oxygen saturation is obtained at the 4x magnification.

The effect of increased oxygen inhaled on hemoglobin oxygen saturation was observed by the switching the air that was inhaled by the mouse from 20% oxygen to 100% oxygen. First 20% oxygenated air was attached to the anesthesia chamber and images were obtained and afterwards the images from 100% oxygenated air were taken.

Glucose Metabolism Measurement

The glucose metabolism was measured while the tumor size is still small or approximately 8mm³. 2-NBDG, a fluorescent analog of glucose is injected intravenous of the mouse tail. The molecule is excited at 470 nm and emits at 535 nm. The mercury lamp of the fluorescent microscope is turned on approximately 15 minutes before imaging, although it is preferable for it to be on at least 30 minutes to allow the lamp to reach its maximum intensity. Hemoglobin oxygen saturation images were taken before the fluorescence imaging. The microscope was changed to the correct filter and the imaging wavelength was set to 525nm. Exposure time remained constant for the duration of the imaging. Once the microscope was set, the mouse was placed on the stand like in trans-illumination imaging and the 2-NBDG was injected. Images were obtained once every second for the first 10 minutes, once every 1 minute for the next 35 minutes, and every 5 minutes for the remaining 30 minutes for a total imaging time of 75 minutes.

Results and Discussion

Non-metastatic tumors exhibited decreased hemoglobin oxygen saturation and increased glucose uptake

Figure 3. presents the representative images of hemoglobin oxygen saturation on days 3, 5 and 7. The images show the tortuousness of the vasculature surrounding the tumor and the increased hemoglobin oxygen saturation of the arteries (thin vessels) compared to the veins (thick vessels). This concept matches literature as arteries carry oxygenated blood to the tissue while veins transport deoxygenated blood away from the tissue.

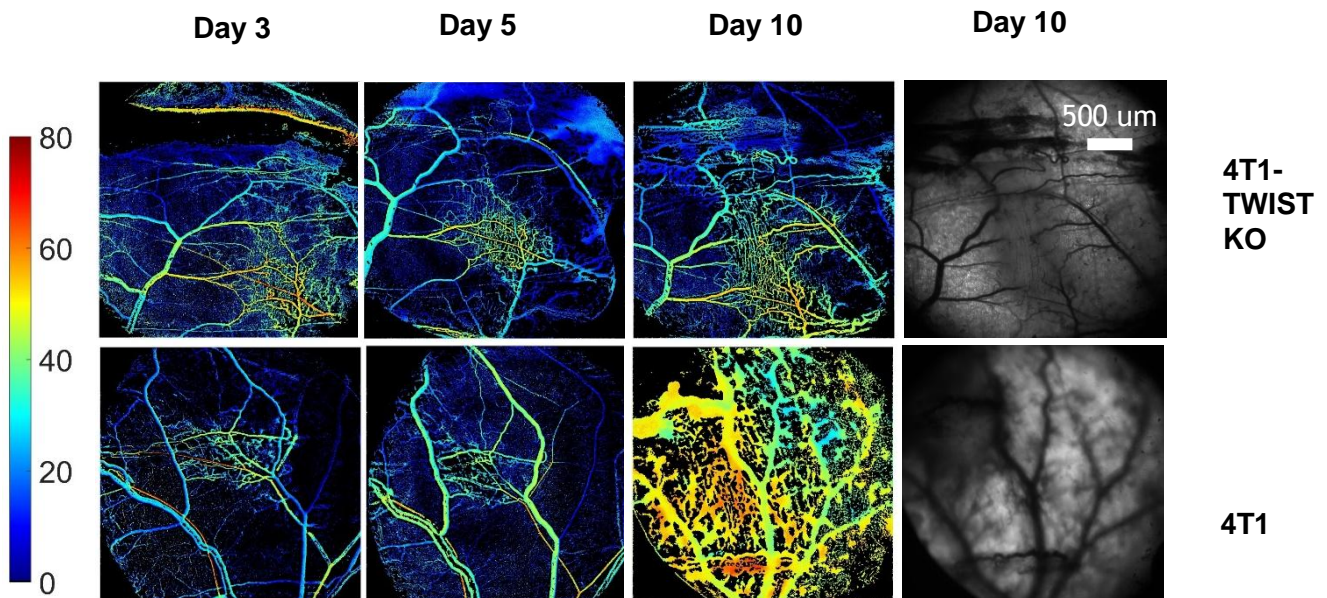


Figure 3. Representative images of hemoglobin oxygen saturation of non-metastatic and metastatic tumors on day 5. Last column of images shows trans-illumination images at 550 nm wavelength of light.

Although from the images it seems as though the 4T1-TWIST KO, the metastatic tumor grew larger and has greater angiogenesis, the average hemoglobin oxygen saturation between all of the mice suggests that the metastatic 4T1 tumors have increased hemoglobin oxygen saturation as the tumor grows.

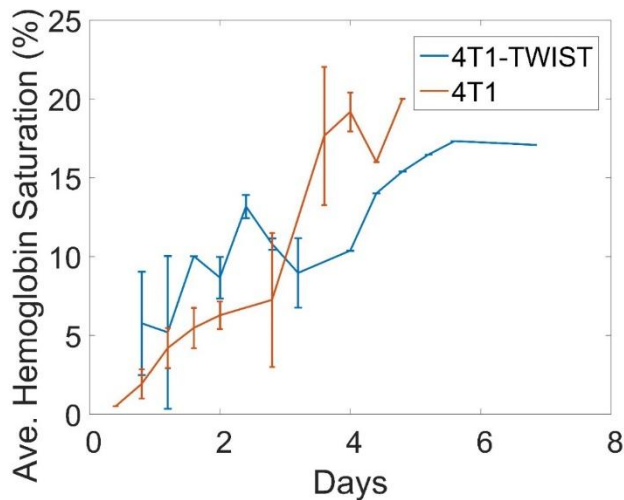


Figure 4. Mean and standard error of hemoglobin oxygen saturation on different days post cell injection, sample size for TWIST and 4T1 are n=2 & 4 respectively. After day 3, 4T1 tumors have increased saturation, n=6.

Figure 4. displays the average hemoglobin oxygen saturation between the metastatic and non-metastatic tumors. The data suggests that initially the non-metastatic tumors have increased hemoglobin oxygen saturation, however, after around day three the metastatic tumors have increased oxygen saturation. This information cannot be fully confirmed as the sample size was 2 for the non-metastatic tumor, and 4 for the metastatic.

Since previous studies have indicated that some metastatic tumors are hypoxic and thus have a low oxygenated tumor microenvironment; therefore, we expected to observe decreased hemoglobin oxygen saturation for the metastatic tumors¹¹. However,

one reason for the increased oxygen saturation can be that since metastatic tumors need to perform more work, they require more ATP. Therefore, they perform oxidative phosphorylation, which is a more efficient pathway for producing energy than glycolysis. If this theory is correct, decreased glucose consumption should be observed by the metastatic tumors.

Figure 5. displays the changes in glucose uptake over a period of 60 minutes at 15 minute intervals. The images suggest that glucose consumption is high initially and then gradually starts decreases. In addition, the data supports the previous hypothesis that the metastatic tumor will have decreased glucose uptake because it performs oxidative phosphorylation. However, the sample size for each tumor is only 1, therefore our hypothesis cannot be confirmed.

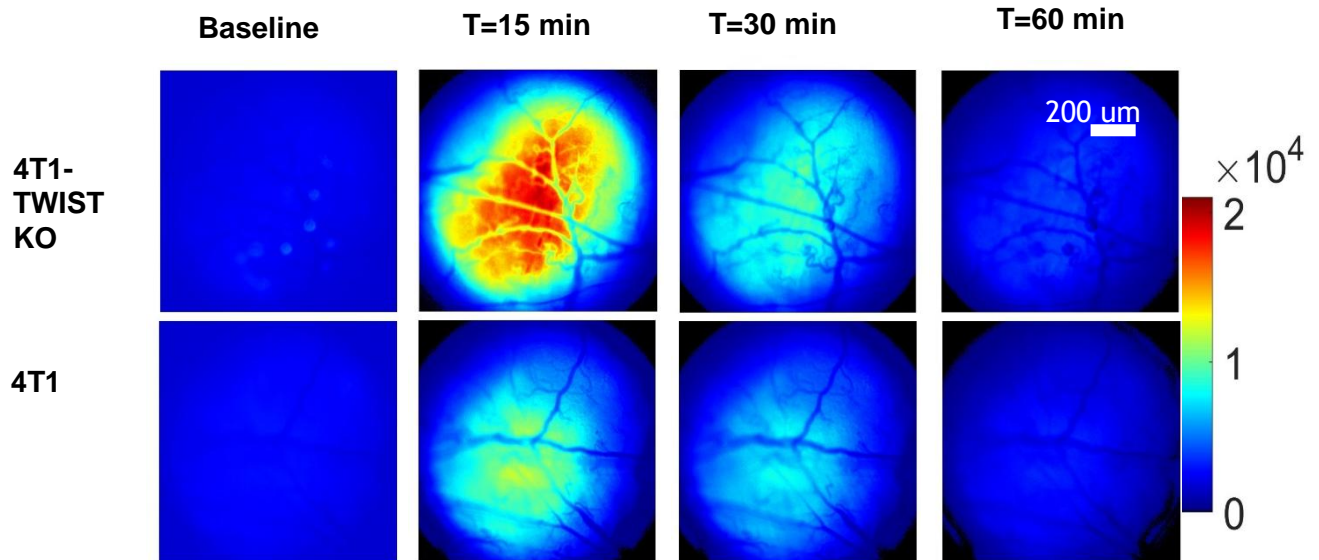


Figure 5. Representative images of 2-NBDG fluorescence of non-metastatic and metastatic tumors on day 5 at different time post injection.

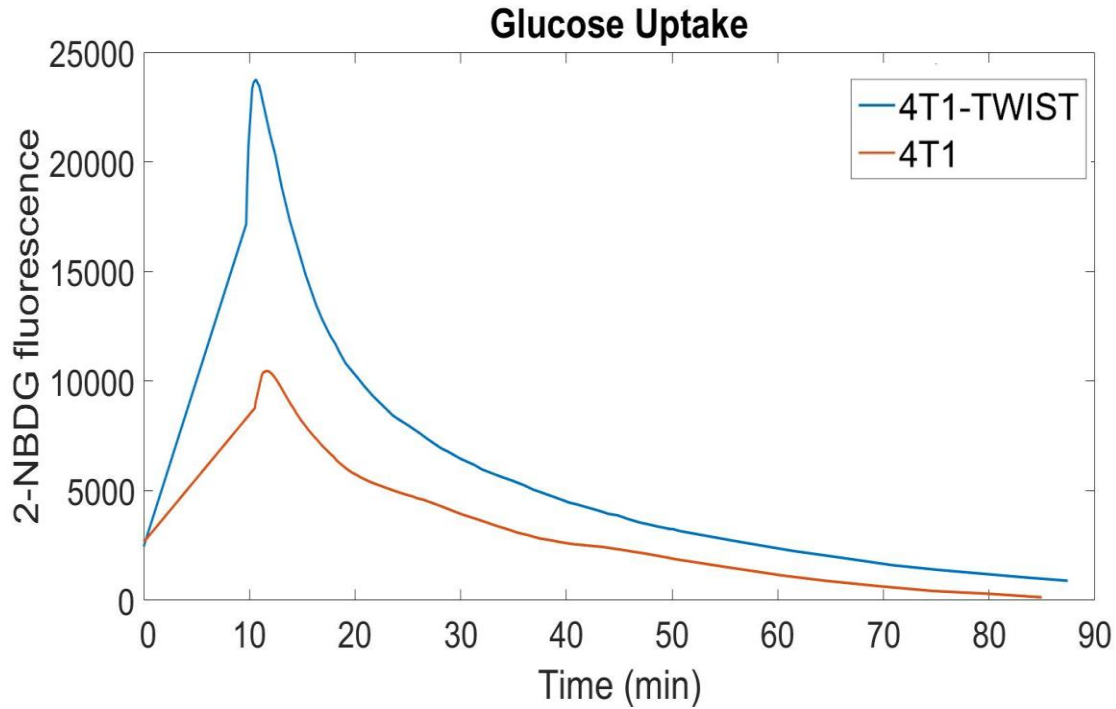


Figure 6. Glucose uptake increases for first 10 mins, then decreases; maximum uptake at ~11 mins; n=2.

Figure 6 displays a graph of the 2-NBDG fluorescence which indicates that initially fluorescence is low. At approximately 13 minutes after injection, the fluorescence reaches a peak, which suggests that the vasculature surrounding the tumor is saturated with 2-NBDG. After 13 minutes, the fluorescence decreases gradually which indicates that glucose is being transported into the tumor. After about 85 minutes, glucose is cleared from the tumor field of view.

Overall, preliminary studies suggest that 4t1-TWIST KO tumors had increased glucose metabolism and decreased oxygenation than the metastatic 4T1 tumors. The decreased need for glucose uptake might be caused by increased oxygenation or more efficient catabolism of glucose. One way to confirm that the 4T1 tumors under more oxidative

phosphorylation than 4T1-TWIST KO is to measure the redox ration of the two tumors and compare them.

Reflectance imaging shows decreased resolution of tumor vasculature compared with transmission imaging at 10x & 20x magnification

Figure 7. displays reflection and transmission mode images of 4T1 tumor of the same field of view and day with different magnifications. The images between the two modes seem to be similar. However, within the red circles, groupings of saturated pixels are observed in the reflection mode.

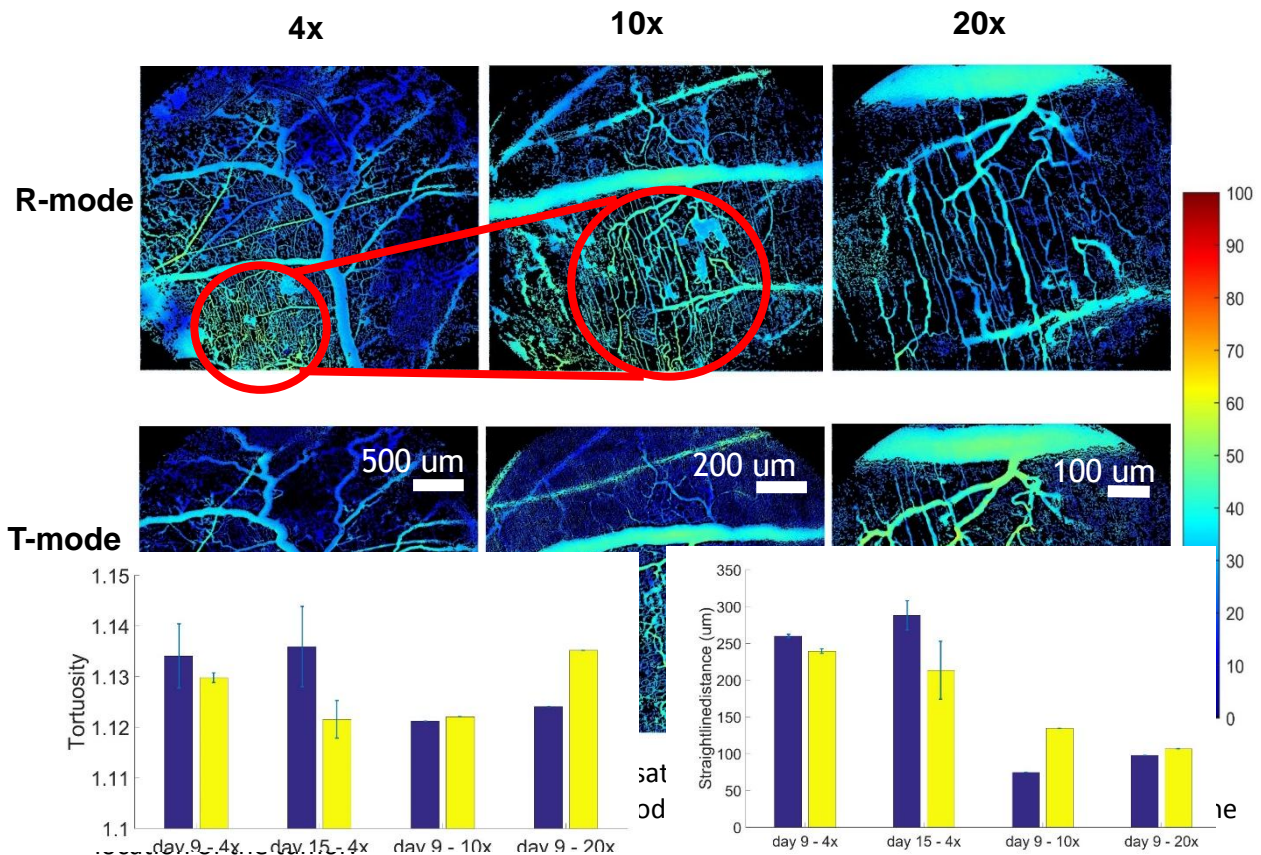


Figure 8. Standard error and means of parameters such as blood vessel tortuosity, mean straight line distance, and branch points of tumor microvasculature compared between 3 magnifications at different days; Sample size for each group is n=2, 2, 1 & 1 respectively.

Measurement of the parameters, from Figure 6., between the two modes of imaging indicate that at 4x magnification, the values of parameters such as tortuosity, mean straight line distance and branch points of tumor vasculature is similar and standard error also appears to be low. However, the values of parameters differ greatly at 10x and 20x magnifications. A small sample size of 2 and 1 for the 4x and 10/20x magnifications makes this data inconclusive, so preliminary studies suggest that reflection mode might have decreased resolution to transmission mode at higher magnifications.

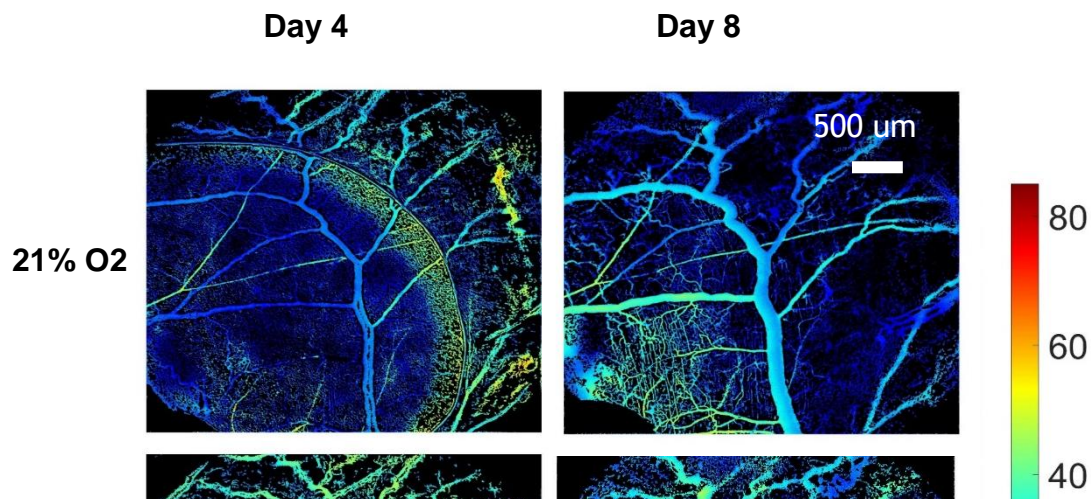
Resolution in measuring parameters such as tortuosity, mean straight line distance and branch points of tumor vasculature is lost when tumors are imaged at reflection mode in higher magnifications than at transmission mode. The decreased resolution might be caused by light reflecting of the glass coverslip that is protecting the tumor from the outside environment. However, at 4x magnification, reflection mode has the better resolution of tortuosity, mean straight line distance, and vasculature branchpoints. As the tumor grows bigger the difference in the values between reflection and transmission increases. For example, at day 9, the values between reflection and

transmission mode are quite similar for all three parameters. The values of the parameters between reflection and transmission images, however, are further apart on day 15 than on day 9. The sample size of this data is two, therefore, it is inconclusive.

Inhaling 100% O₂ increases hemoglobin oxygen saturation

Figure 9. indicates that when inhaling 100% oxygenated air, the hemoglobin oxygen saturation measured has increased compared to inhaling 21% oxygenate air. The vessels have increased intensity of oxygen saturation and the microvasculature around the tumor also had increased saturation. The bar graph in Figure 10. quantifies the hemoglobin oxygen saturation and indicates that oxygen saturation is approximately 11% on day 4 and 29% on day 8. When 100% oxygenated air in breathed in the hemoglobin oxygen saturation by around 10% on both days. This data shows that inhaling more oxygen can increase oxygenation of the tumor microvasculature by approximately 10%.

Overall, the hemoglobin oxygen saturation increased when 100% oxygen, rather than room air (21% oxygen), was inhaled by the mouse while it was under anesthesia. The tumor oxygenation also increased as the 4T1 tumor grew.



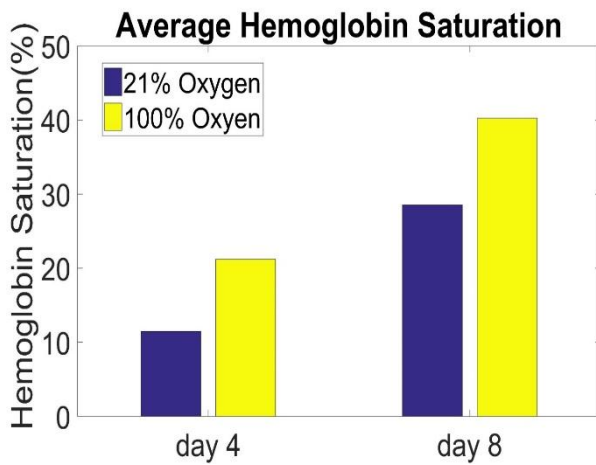


Figure 10. Hemoglobin oxygen saturation from 21% to 100% oxygen inhalation and on different days post cell injection, each of size n=1. Hemoglobin oxygen saturation increases by a factor of 2 on day 4, and 0.33 on day 8.

Conclusions

We initially set out to set out a base for diagnosing metastatic tumors from non-metastatic tumors. Our hypothesis was that the metastatic 4T1 tumors will exhibit

increased glucose metabolism and decreased oxygen saturation than the non-metastatic 4T1-TWIST KO tumors, as indicated by previous studies. For this reason, we measured glucose consumption through fluorescence imaging of an analog of glucose (2-NBDG) and hemoglobin oxygen saturation through hyperspectral trans-illumination imaging of the tumor from 520 to 620nm. The data rejected our hypothesis and suggests that metastatic tumors exhibit increased oxygen saturation and decreased glucose metabolism than non-metastatic tumors. Enhanced efficiency in producing ATP through oxidative phosphorylation rather than glycolysis could be explain the phenomena that observed. However, further studies are required to identify increased oxidative phosphorylation of the metastatic tumors.

We also wanted to identify whether reflection mode and transmission imaging modes can give similar images, as it is important to be able have both modalities on a microscope and be able to image the same field of view. The preliminary studies indicate that reflection and transmission mode product similar measurements at 4x magnification, although with the increased presence of saturated pixels in the reflection mode. At 10x and 20x magnifications, reflection mode outputs vary greatly from transmission mode, and might not be able to pick up intricacies in tumor microvasculature. However, a small sample size makes it difficult to confirm this conclusion.

Lastly, we wanted to observe the effect of breathing in 100% oxygenated air rather than 21% on the measured hemoglobin oxygen saturation. The data follows what was expected, because inhaling in 100% O₂ increased the hemoglobin oxygen

saturation by approximately 10% on day 4 and 8. A greater sample size will further support this conclusion.

Future Directions

Future studies include including repeating the study with a greater sample size to conclusively see whether metastatic tumors might perform more oxidative phosphorylation than non-metastatic tumors and ultimately developing a prognosis model for metastatic breast tumors. One method of comparing oxidation phosphorylation performance between the two cell lines is to obtain the redox ratio. The redox ratio is pixel-wise ratio of flavin adenine dinucleotide (FAD) molecules to nicotinamide adenine dinucleotide (NADH) and FAD molecules¹. NADH and FAD are endogenous fluorophores that are components of the cellular respiration pathway. Glycolysis produces 2 NADH and the citric acid cycle produces 6 NADH and FADH₂ molecules. Oxidative phosphorylation uses up the NADH and FAD molecules to make ATP. Thus, a redox ratio close to 1 would indicate more oxidative phosphorylation taking place. Therefore, future studies include fluorescence imaging the NADH and FAD of the tumors and also observing how, glucose metabolism, oxidative phosphorylation, and hemoglobin oxygen saturation change as the tumor is put through hypoxia.

References

1. Alhallak, Kinan et al. "Optical Redox Ratio Identifies Metastatic Potential-Dependent Changes In Breast Cancer Cell Metabolism". *Biomedical Optics Express* 7.11 (2016): 4364.
2. Valastyan, Scott, and Robert A. Weinberg. "Tumor Metastasis: Molecular Insights And Evolving Paradigms". *Cell* 147.2 (2011): 275-292.
3. Richards, Mike and Clare Gerada. "Improving Outcomes: A Strategy for Cancer". Department of Health (2011). Webinar
4. Beckmann, Matthias W., and Michael P. Lux. "Health Economics In Breast Cancer". *Breast Care* 8.1 (2013): 5-6.
5. Lyman, Gary H. "Economics of Cancer Care". *Journal of Oncology Practice* (2007) 3:3, 113-114.
6. Rajaram, Narasimhan et al. "Delivery Rate Affects Uptake Of A Fluorescent Glucose Analog In Murine Metastatic Breast Cancer". *PLoS ONE* 8.10 (2013): e76524.
7. Krzeslak, Anna et al. "Expression Of GLUT1 And GLUT3 Glucose Transporters In Endometrial And Breast Cancers". *Pathology & Oncology Research* 18.3 (2012): 721-728.
8. Embley, T. M., & Martin, W. (2006). Eukaryotic evolution, changes and challenges. *Nature*, 440(7084), 623-630. doi:10.1038/nature04546
9. Gatenby, Robert A., and Robert J. Gillies. "Why Do Cancers Have High Aerobic Glycolysis?". *Nature Reviews Cancer* 4.11 (2004): 891-899.

10. Gilkes, Daniele M., Gregg L. Semenza, and Denis Wirtz. "Hypoxia And The Extracellular Matrix: Drivers Of Tumour Metastasis". *Nature Reviews Cancer* 14.6 (2014): 430-439.
11. Melillo, Giovanni. "Targeting Hypoxia Cell Signaling For Cancer Therapy". *Cancer and Metastasis Reviews* 26.2 (2007): 341-352.
12. Nitzan, M., Romem, A., & Koppel, R. (2014). Pulse oximetry: Fundamentals and technology update. *MDER Medical Devices: Evidence and Research*, 231.
13. Palmer, Gregory M. et al. "Optical Imaging Of Tumor Hypoxia Dynamics". *Journal of Biomedical Optics* 15.6 (2010): 066021.

Acknowledgements

This project was performed under the guidance and mentorship of Dr. Narasimhan Rajaram and with the provision of materials through his laboratory. Additional support and funding was provided by the University of Arkansas Honors College Research Grant.